Design and analysis of a highly efficient coupler between a micro/nano optical fiber and an SOI waveguide

Zehua Hong,[1] Linjie Zhou,[1] Xinwan Li,[1,2,*] Weiwen Zou,[1] Xiaomeng Sun,[1] Shuguang Li,[1] Jianguo Shen,[1] Haimei Luo,[1] and Jianping Chen[1]

[1]State Key Laboratory of Advanced Optical Communication Systems and Networks, Department of Electronic Engineering, Shanghai Jiao Tong University, Shanghai 200240, China

[2]School of Physics and Electrical Information Science, Ningxia University, Ningxia 750021, China

*Corresponding author: lixinwan@sjtu.edu.cn

Received 6 January 2012; revised 7 March 2012; accepted 13 March 2012; posted 15 March 2012 (Doc. ID 160926); published 30 May 2012

A compact coupling structure is proposed for highly efficient coupling between a micro/nano fiber and a silicon-on-insulator waveguide. The proposed structure is characterized by high coupling efficiency, wavelength insensitivity, large misalignment tolerance, and easy fabrication. Theoretical analysis and numerical simulation results show that coupling efficiency of >90% can be achieved with a taper length of ~4.5 μm. © 2012 Optical Society of America

OCIS codes: 060.2340, 230.4000, 050.6624.

1. Introduction

Recently, optical interconnects and optical network-on-chips (ONoCs) have attracted much research interest [1,2]. Low-cost and compact optical modules are required for these optical networks. Silicon photonics is one of the most promising technologies that can be applied to the ONoCs because of the small footprint of silicon photonic devices and their compatibility with conventional complementary metal-oxide semiconductor (CMOS) fabrication techniques. Optical packaging is crucial for a reliable optical module. However, efficient light coupling between single-mode fibers (SMFs) and silicon-on-insulator (SOI) waveguides is a great challenge because of the mismatch between their mode profiles and effective refractive indices, resulting in radiation loss and back reflection loss [3].

Various approaches have been proposed to improve the coupling efficiency between SMFs and SOI waveguides, such as adiabatic tapering (including normal and invert tapering) [4–6], grating-assisted coupling [7–9], and graded-index (GRIN) lens [10]. An inverted adiabatic taper is used to effectively transform both the mode field profile and the effective refractive index between an SMF and an SOI waveguide, but usually a long taper length (>40 μm) is needed. Moreover, the taper tip needs to be tiny, which imposes a great challenge for the alignment [6]. A double-stage adiabatic taper structure has also been proposed, which uses a larger aperture taper to alleviate the stringent alignment. However, the fabrication process for such structures is complicated, and a long taper length (>1000 μm) is always required [4]. Grating coupler is one of the most efficient coupling structures. Wang *et al.* demonstrated a nonuniform grating coupler with a 68% coupling efficiency [11]. Although the grating-assisted coupling scheme can relax the stringent alignment, their coupling efficiency is wavelength-dependent, and the 3-dB bandwidth is relatively narrow [11], thereby limiting their use. GRIN lens can also be used for mode-size conversion on a similar principle with graded-index fibers.

1559-128X/12/163410-06$15.00/0
© 2012 Optical Society of America

The GRIN lens shows a fairly collimated character, but the fabrication process is very complicated and the structure is not compact [10].

Micro/nano optical fibers (MNOFs) exhibit a number of exciting properties, such as large evanescent field and strong optical confinement [12,13]. When the diameter of an SMF decreases to micro/nano scale, a considerable fraction of light is localized outside the fiber, which can be used to realize highly efficient evanescent coupling in a short coupling length. In this paper, we propose a compact coupling structure for highly efficient coupling between an MNOF and an SOI waveguide.

2. Device Structure

Figure 1 shows the schematic drawings of our proposed coupling structure for three different views. The MNOF with a diameter of ~800 nm (refractive index $n_{\mathrm{MNOF}} = 1.45$ nm at 1550 nm) is drawn from an SMF by using hydrogen heating [14]. The diameter along the longitudinal direction of the MNOF is usually nonuniform. However, in our structure, because the overlap length between the MNOF and the SOI waveguide is only within 10 μm, the MNOF radius nonuniformity is less than 17 nm, which is negligible. The width of the SOI waveguide ($n_{\mathrm{si}} = 3.48$ at 1550 nm) is tapered from 450 nm down to a tip width of 200 nm, and the height remains constant at 250 nm. We design two SiO_2 ($n_{SiO_2} = 1.45$ at 1550 nm) strips standing on both sides of the SOI waveguide with a height of 650 nm, which play a similar role as V-grooves in fiber packaging. The spacing between these two strips is equal to the diameter of the MNOF. The width of the SiO_2 strips is also tapered from ~500 nm to ~300 nm to push the light into the SOI waveguide. The undercladding SiO_2 layer thickness is assumed to be 3 μm to prevent light leakage to the silicon substrate. In our simulation, light is input from the MNOF and then coupled to the SOI waveguide. The output power from the end of the SOI waveguide is collected. The coupling efficiency is evaluated as $\eta = P_{\mathrm{out}}/P_{\mathrm{in}}$, where P_{in} and P_{out} are the input and output optical power, respectively.

Coupled-mode theory is routinely employed for weakly coupled structures. However, in our proposed structure, the evanescent field becomes so strong that the errors associated with the coupled-mode theory can no longer be negligible [15,16]. To accurately model the coupling behavior, one can use the following two methods: one is the strongly coupled-mode theory [17], and the other is to directly solve Maxwell's equations using a numerical method, such as the finite-difference time-domain method [18] and the finite element method (FEM) [19]. In the following sections, we first analyze the coupling characteristics of the structure by using strongly coupled-mode theory, and we then analyze in detail the parameter dependence of the coupling efficiency using the finite element method.

3. Theoretical Analysis with the Strongly Coupled-Mode Theory

For two parallel uniform waveguides, the light field propagation equation based on the strongly coupled-mode theory can be written as [17]

$$\frac{d}{dz}\begin{bmatrix} a(z) \\ b(z) \end{bmatrix} = j \cdot \begin{bmatrix} \gamma_a & K_{ab} \\ K_{ba} & \gamma_b \end{bmatrix} \begin{bmatrix} a(z) \\ b(z) \end{bmatrix}, \tag{1}$$

where $a(z)$ and $b(z)$ are the z-dependent amplitudes of the individual guided modes. The propagation constants γ_a and γ_b are given by

$$\gamma_a = \beta_a + (\tilde{K}_{aa} - C_{ab}\tilde{K}_{ba})/(1 - C_{ab}C_{ba}), \tag{2a}$$

$$\gamma_b = \beta_b + (\tilde{K}_{bb} - C_{ba}\tilde{K}_{ab})/(1 - C_{ab}C_{ba}), \tag{2b}$$

where β_a and β_b describe the individual waveguide mode propagation constants. The coupling coefficients are

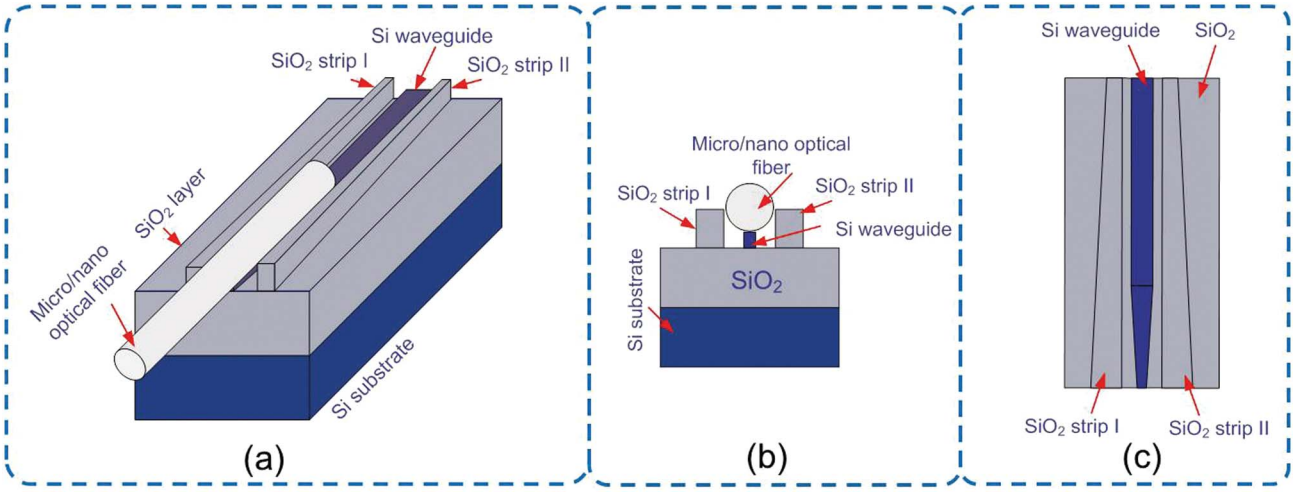

Fig. 1. (Color online) Schematic illustration of the coupling scheme between an MNOF and a tapered SOI waveguide. (a) 3D view; (b) cross-sectional view; (c) top view.

$$K_{ab} = (\tilde{K}_{ab} - \tilde{K}_{bb}C_{ab})/(1 - C_{ab}C_{ba}), \tag{3a}$$

$$K_{ba} = (\tilde{K}_{ba} - \tilde{K}_{aa}C_{ba})/(1 - C_{ab}C_{ba}). \tag{3b}$$

In Eqs. (2a)–(3a), $\tilde{K}_{pq}(p,q = a,b)$ is the perturbation between two waveguides, and $C_{pq}(p,q = a,b)$ is the waveguide mode overlap. If C_{pq}, $\tilde{K}_{aa}$ and $\tilde{K}_{bb}$ become zero, Eq. (1) describes weak coupling.

Equation (1) is applicable to the coupling between two parallel uniform waveguides. For the tapered waveguide used in our coupling structure, the stepwise approximation is made for the theoretical analysis, as shown in Fig. 2 [20]. Within each step, Eq. (1) can be used. Based on the stepwise model, we obtain the relationship

$$\begin{bmatrix} a(z) \\ b(z) \end{bmatrix} = \left(\prod_n M_n\right) \exp(j\varphi(z)) \begin{bmatrix} a(0) \\ b(0) \end{bmatrix}, \tag{4}$$

where

$$M_n = \begin{bmatrix} \cos(\psi_n dz) - j\frac{\Delta_n}{\psi_n}\sin(\psi_n dz) & j\frac{K_{ab}^{(n)}}{\psi_n}\sin(\psi_n dz) \\ j\frac{K_{ba}^{(n)}}{\psi_n}\sin(\psi_n dz) & \cos(\psi_n dz) + j\frac{\Delta_n}{\psi_n}\sin(\psi_n dz) \end{bmatrix}, \tag{5}$$

$$\psi_n = \sqrt{\Delta_n^2 + K_{ab}^{(n)}K_{ba}^{(n)}}, \tag{6a}$$

$$\Delta_n = \frac{\gamma_b^{(n)} - \gamma_a^{(n)}}{2}, \tag{6b}$$

where $\varphi(z)$ is the z-dependent phase shift. M_n represents the transfer matrix of the nth step.

Solving Eqs. (2a)–(6b), we can get the energy flow in the two waveguides. For simplicity, we assume $\Delta_n = -45.16 \cdot \delta n_{\text{eff}}(n)$, $K_{ba}^{(n)} = 1.96 - 0.4 \cdot \delta n_{\text{eff}}(n)$, and $K_{ab}^{(n)} = 3.84/K_{ba}^{(n)}$ change linearly with the effective refractive index difference (δn_{eff}) between the two waveguides [17], $\delta n_{\text{eff}}(n+1) = \delta n_{\text{eff}}(n) - 0.193 \cdot dz$ and $\delta n_{\text{eff}}(0) = n_{\text{eff MNOF}}(0) - n_{\text{eff SOIwaveguide}}(0) = 0.091$. Although the two silica strips also take part in the coupling, the coupling mainly occurs between the MNOF and the SOI tapered waveguide. For simplicity, we consider only the coupling between the MNOF and the SOI waveguide in this section. With the above assumptions, we get the optical power flow as shown in Fig. 3. The solid curve is for the coupling between the MNOF with a diameter of 800 nm and the tapered SOI waveguide, as described in Section 2. It shows when the width of tapered waveguide increases gradually, most of the energy will be transferred from the MNOF to the SOI waveguide. When the SOI waveguide width gradually increases, the propagation constants γ_a and γ_b approach each other in some steps, and as a result, optical energy is rapidly transferred to the SOI waveguide. As the waveguide width keeps increasing, optical energy cannot be transferred back and remains in the SOI waveguide. In contrast, if the SOI waveguide width is uniform, their propagation constants will be mismatched, and therefore it is hard to couple optical power from one waveguide into another, as shown by the dash curve in Fig. 3. In this case, the coupling efficiency is as low as ~1%.

Strongly coupled-mode theory can provide a first glance of the coupling characteristics, but it is still an approximate method. In order to more accurately analyze our complex coupling structure, numerical simulation methods are used.

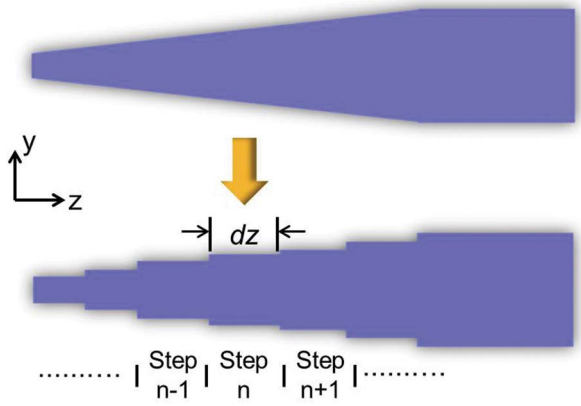

Fig. 2. (Color online) Stepwise approximation used in our theoretical analysis.

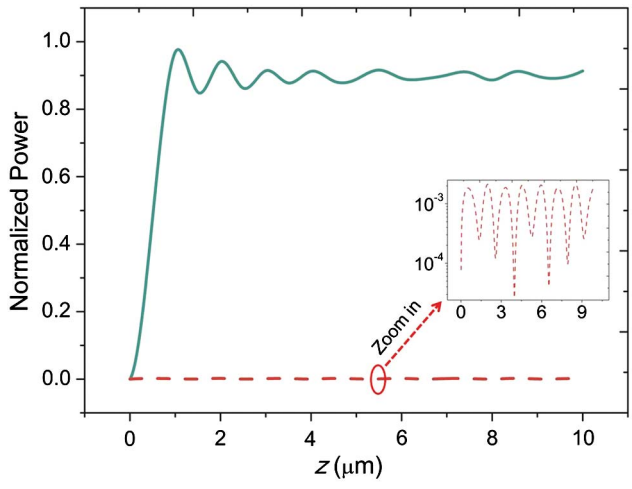

Fig. 3. (Color online) Optical power distribution along z direction in the SOI waveguide (input from the MNOF). Optical power is normalized to input power. Solid curve is for the tapered SOI waveguide, and dashed curve for uniform SOI waveguide.

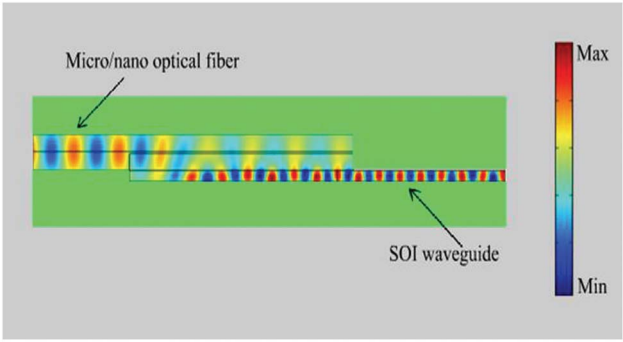

Fig. 4. (Color online) Optical power flow pattern (Media 1) in the MNOF and SOI waveguide.

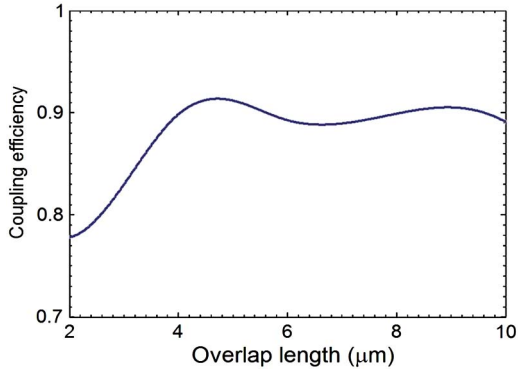

Fig. 6. (Color online) Coupling efficiency changes as a function of overlap length between the MNOF and the SOI waveguide.

4. Numerical Simulations

In this section, we analyze the effects of MNOF and SOI waveguide geometrical parameters on the coupling efficiency by using commercial the 3D FEM software COMSOL Multiphysics [19]. In the analysis, we change one of the parameters and fix the others. It should be noted that, to obtain more accurate results, the coupling effect of silica strips is taken into account in this section.

Figure 4 (Media 1) intuitively illustrates the optical energy flow between the MNOF and the SOI waveguide. The overlap length between them is 10 μm, and the SOI taper length is 6.5 μm. Other geometrical parameters are the same as those used in Section 2. Figure 4 clearly shows that the optical energy is transferred from the MNOF (with a diameter of 800 nm) to the tapered SOI waveguide in a very short length, similar to the results obtained from the strongly coupled-mode theory.

Figure 5 shows the coupling efficiency changes as a function of wavelength. It shows that the proposed coupler has a relatively flat coupling efficiency over a wide wavelength range. Similar to our previous work [19], the coupling efficiency is also overlap-length-dependent, as shown in Fig. 6. When the overlap length increases to about 5 μm, the coupling efficiency reaches the maximum of >91%. When the overlap length further increases, the coupling efficiency remains almost stable, around 90%, which implies that as long as the overlapping length exceeds a certain value, we can always get a stable high coupling efficiency. With such a feature, there is no need to accurately set the overlap length, as opposed to the conventional directional couplers.

The taper length and tip width are another two key parameters in getting a high coupling efficiency. From Figs. 7 and 8, we can see that a high coupling efficiency of >90% can be obtained when the taper length varies from 4 to 6 μm and tip width varies from 100 to 160 μm. The optimum parameters are 4.5 μm for the taper length and 145 nm for the tip width. Figure 7 indicates that the coupling efficiency is sensitive to the taper length. With a short taper length, high-order modes of the SOI waveguide are excited, which causes a fast deterioration in coupling efficiency. In contrast, when the taper length is long, the tapered SOI waveguide cannot confine light well. As a result, a considerable amount of light is coupled to the underlying SiO_2 layer, which also lowers the coupling efficiency. The coupling efficiency degradation is acceptable when the variation in taper length is within ± 1 μm, as shown in Fig. 7. The waveguide end tip size can also affect the coupling efficiency. A tiny tip makes the fabrication difficult, but a wide tip induces a larger reflection. In comparison, the coupling efficiency is less sensitive to the tip width than to the taper length, as shown in Fig. 8. In a relatively wide range (100–200 μm), the coupling efficiency degradation is acceptable.

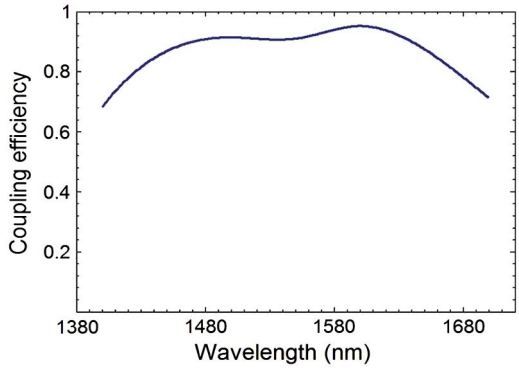

Fig. 5. (Color online) Coupling efficiency changes as a function of wavelength.

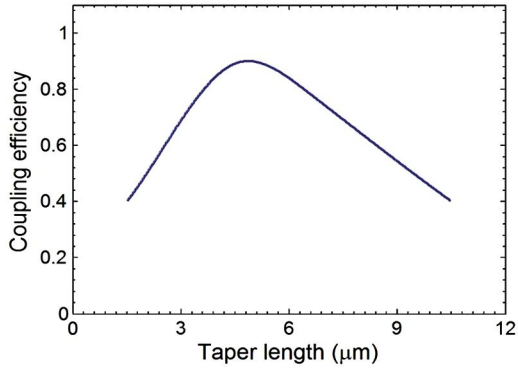

Fig. 7. (Color online) Coupling efficiency changes as a function of taper length.

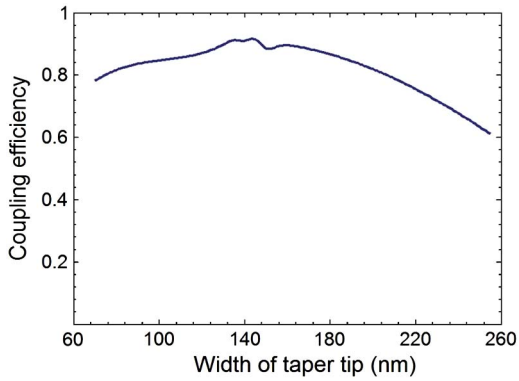

Fig. 8. (Color online) Coupling efficiency changes as a function of taper tip width.

The purpose of the two SiO_2 strips is to fix the MNOF and align it with the SOI waveguide. If the separation between the two SiO_2 strips is larger/smaller than the diameter of the MNOF, lateral/vertical misalignment occurs, lowering the coupling efficiency. Figure 9(a) shows that the coupling efficiency degradation induced by lateral misalignment is very small. A ±80 nm lateral misalignment only lowers the coupling efficiency by ~10%. Figure 9(b) shows that the vertical separation of <120 nm between the MNOF and the SOI waveguide does not significantly degrade the coupling efficiency. However, when the vertical separation exceeds 120 nm, the coupling efficiency deteriorates significantly to

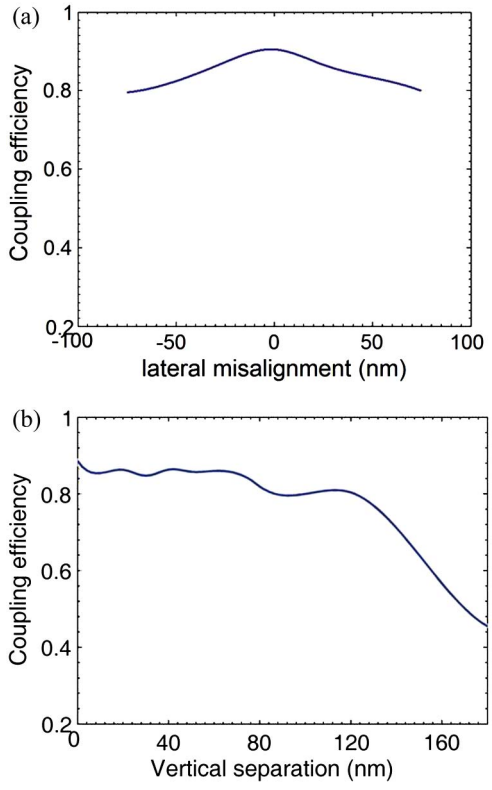

Fig. 9. (Color online) Coupling efficiency changes as a function of (a) lateral and (b) vertical misalignment.

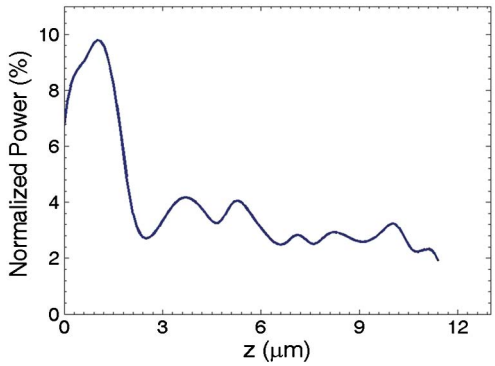

Fig. 10. (Color online) Optical power distribution along z direction in one of the silica strips. Power is normalized by input power.

only 50%, for a separation of 170 nm. Considering that light propagating in the MNOF can be coupled to the two SiO_2 strips to decrease the coupling efficiency, we also taper the SiO_2 strips along the longitudinal direction, which can compel most of the light back to the SOI waveguide. The optical power distribution along the z direction of silica strips is shown in Fig. 10. At the beginning, only ~10% of the optical power is transferred to one of the silica strips at $z = 1$ μm, and then the transferred power is rapidly reduced to ~3%. At the end, only ~2% of the power remains in one of the silica strips. Figure 10 also justifies the assumption, made in Section 3, that the coupling mainly occurs between the MNOF and the SOI tapered waveguide.

5. Discussion

By optimizing the device geometrical parameters, we can get a maximum coupling efficiency of >91% when the taper length, tip width, and overlapping length are 4.5 μm, 145 nm, and 5 μm, respectively. In practice, it is very difficult to get the exact optimal geometrical parameters. However, the proposed structure has a good error tolerance, as shown in Figs. 5–9, and the current fabrication techniques can fully satisfy the requirement. For the MNOF, we have developed a homemade setup to fabricate the low-loss MNOFs with the diameter and uniformity controllable [14,19]. With regard to the overlap length between the MNOF and SOI waveguide, as the simulation result shows, once the overlap length exceeds a certain value, the coupling efficiency becomes stable and only fluctuates slightly, which releases the requirement for stringent alignment. The SOI waveguide can be fabricated using current CMOS fabrication techniques with its dimensions controlled within several nanometers, which can fully meet our device error-tolerance requirement. Our next step is to fabricate and demonstrate such structures in experiment.

6. Conclusion

We have proposed and numerically analyzed a compact coupling structure for highly efficient coupling between an MNOF and an SOI waveguide. The simulation results show that the coupling efficiency

can be larger than 90% for a coupling length of only ~5 μm. The structure has a good error tolerance, which can relax the requirement for accurate alignment. The highly efficient and compact coupling structure proposed in this paper is feasible. Our next step is to fabricate and demonstrate such structures in experiment. We believe the proposed coupling structure can be used for optical packages of silicon photonic chips.

This work was supported in part by 973 program (ID2011CB301700), International Cooperation Project from Ministry of Science and Technology, China (2011FDA11780), NSFC (60877012, 61007039, 61007052, 61107041, 61127016), STCSM Project (10DJ1400402, 09JC1408100), State Key Lab Projects (GKZD030004/09/15/20/21), Shanghai Jiao Tong University Innovation Fund For Postgraduates.

References

1. N. Sherwood-Droz, H. Wang, and L. Chen, "Optical 4 × 4 hitless silicon router for optical networks-on-chip (NoC)," Opt. Express **16**, 15915–15922 (2008).
2. M. Yang, W. M. J. Green, and S. Assefa, "Non-Blocking 4 × 4 electro-optic silicon switch for on-chip photonic networks," Opt. Express **19**, 47–54 (2011).
3. L. Vivien, X. Le Roux, and S. Laval, "Design, realization, and characterization of 3-D taper for fiber/micro-waveguide coupling," IEEE J. Sel. Top. Quantum Electron. **12**, 1354–1358 (2006).
4. A. Barkai, A. Liu, D. Kim, and R. Cohen, "Double-Stage taper for coupling between SOI waveguides and single-mode fiber," J. Lightwave Technol. **26**, 3860–3865 (2008).
5. K. K. Lee, D. R. Lim, D. Pan, and C. Hoepfner, "Mode transformer for miniaturized optical circuits," Opt. Lett. **30**, 498–500 (2005).
6. V. R. Almeida and R. R. Panepucci, "Nanotaper for compact mode conversion," Opt. Lett. **28**, 1302–1304 (2003).
7. B. Wang, J. Jiang, D. M. Chambers, and J. Cai, "Stratified waveguide grating coupler for normal fiber incidence," Opt. Lett. **30**, 845–847 (2005).
8. G. Roelkens, D. Vermeulen, and D. Van Thourhout, "High efficiency diffractive grating couplers for interfacing a single mode optical fiber with a nanophotonic silicon-on-insulator waveguide circuit," Appl. Phys. Lett. **92**, 131101 (2008).
9. X. Chen, C. Li, and Hon Ki Tsang, "Fabrication-tolerant waveguide chirped grating coupler for coupling to a perfectly vertical optical fiber," IEEE Photon. Technol. Lett. **20**, 1914–1916 (2008).
10. T. H. Loh, Q. Wang, J. Zhu, K. T. Ng, and Y. C. Lai, "Ultra-compact multilayer Si/SiO2 GRIN lens mode-size converter for coupling single-mode fiber to Si-wire waveguide," Opt. Express **18**, 21519–21533 (2010).
11. Z. Wang and Y. Tang, "High efficiency grating couplers for silicon-on-insulator photonic circuits," in *Proceedings of IEEE Conference on Optical Communication* (ECOC, 2010), P2.06.
12. L. Tong, R. R. Gattass, J. B. Ashcom, S. He, J. Lou, M. Shen, I. Maxwell, and E. Mazur, "Subwavelength-diameter silica wires for low-loss optical wave guiding," Nature **426**, 816–819 (2003).
13. L. J. Chen, H. W. Chen, and T. F. Kao, "Low-loss subwavelength plastic fiber for terahertz waveguiding," Opt. Lett. **31**, 308–310 (2006).
14. J. P. Chen, X. Shen, Z. Hong, and X. Li, "Nanostructure optic-fiber-based devices for optical signal processing," in *Proceedings of the 15th OptoElectronics and Communications Conference* (OECC, 2010), 8E2-1.
15. G. H. Wang, P. Shum, G. B. Ren, X. Yu, J. J. Hu, and C. Lin, "Theoretical investigation of nanowaveguide-based optical coupler using mode expansion transfer matrix," Microw. Opt. Technol. Lett. **52**, 1123–1129 (2010).
16. L. Tong, J. Lou, and E. Mazur, "Single-mode guiding properties of subwavelength-diameter silica and silicon wire waveguides," Opt. Express **12**, 1025–1035 (2004).
17. S. L. Chuang, "Application of the strongly coupled-mode theory to integrated optical devices," IEEE J. Quantum Electron. **23**, 499–509 (1987).
18. K. Huang, S. Yang, and L. Tong, "Modeling of evanescent coupling between two parallel optical nanowires," Appl. Opt. **46**, 1429–1434 (2007).
19. Z. Hong, X. Li, and L. Zhou, "Coupling characteristics between two conical micro/nano fibers: simulation and experiment," Opt. Exp. **19**, 3854–3861 (2011).
20. A. R. Nelson, "Coupling optical waveguides by tapers," Appl. Opt. **14**, 3012–3015 (1975).